Virology 489 (2016) 20–33

Contents lists available at ScienceDirect

Virology

journal homepage: www.elsevier.com/locate/yviro

Cytorhabdovirus P3 genes encode 30K-like cell-to-cell movement proteins

Krin S. Mann [a], Nicolas Bejerman [a,1], Karyn N. Johnson [b], Ralf G. Dietzgen [a,*]

[a] Queensland Alliance for Agriculture and Food Innovation, The University of Queensland, St Lucia, QLD 4072, Australia
[b] School of Biological Sciences, The University of Queensland, St Lucia, QLD 4072, Australia

ARTICLE INFO

Article history:
Received 26 August 2015
Returned to author for revisions
25 November 2015
Accepted 26 November 2015
Available online

Keywords:
Lettuce necrotic yellows virus
Alfalfa dwarf virus
Turnip vein-clearing virus reporter replicon
Cell-to-cell movement
30K superfamily
Trans-complementation
Nicotiana benthamiana
Virus–plant protein interactions

ABSTRACT

Plant viruses encode movement proteins (MP) to facilitate cell-to-cell transport through plasmodesmata. In this study, using *trans*-complementation of a movement-defective turnip vein-clearing tobamovirus (TVCV) replicon, we show for the first time for cytorhabdoviruses (lettuce necrotic yellows virus (LNYV) and alfalfa dwarf virus (ADV)) that their P3 proteins function as MP similar to the TVCV P30 protein. All three MP localized to plasmodesmata when ectopically expressed. In addition, we show that these MP belong to the 30K superfamily since movement was inhibited by mutation of an aspartic acid residue in the critical 30K-specific LxD/N_{50-70}G motif. We also report that *Nicotiana benthamiana* microtubule-associated VOZ1-like transcriptional activator interacts with LNYV P3 and TVCV P30 but not with ADV P3 or any of the MP point mutants. This host protein, which is known to interact with P3 of sonchus yellow net nucleorhabdovirus, may be involved in aiding the cell-to-cell movement of LNYV and TVCV.

Introduction

The local spread of viruses in plants is mediated by movement proteins (MP), which ferry infectious genetic material from cell-to-cell through the modification of membrane-lined pores in the cell wall referred to as plasmodesmata (PD) (Ding et al., 1992; Robards and Lucas, 1990; Sevilem et al., 2013). This is exemplified by tobacco mosaic virus (TMV) P30 MP, which was shown to increase PD pore size by nearly 10-fold (Wolf et al., 1989). Following cell-to-cell spread, MP assist in the transport of the viral genome to vascular (phloem) tissues, which in susceptible species leads to systemic spread of virus-like particles (VLPs) and/or virions into the rest of the plant (Ryabov et al., 1998; Scholthof, 2005).

The 30K MP superfamily was recently proposed to be one of the most phylogenetically diverse plant virus gene families (Mushegian and Elena, 2015). These specialized plant viral MP have been shown to similarly facilitate cell-to-cell movement by binding to nucleic acids, localizing to the cell periphery at PD, and increasing PD pore size (Citovsky et al., 1990; Koonin et al., 1991; Melcher, 2000; Oparka et al., 1997; Tomenius et al., 1987; Wolf et al., 1989). In addition, some members of this MP superfamily such as tomato spotted wilt tospovirus NSm can form tubules through PD to facilitate cell-to-cell spread of VLPs (Amari et al., 2010; Kasteel et al., 1996; Storms et al., 1995). Despite a lack of amino acid sequence conservation, one of the defining structural characteristics of 30K-like MP is a common core domain (CCD) that consists of two to four α-helices that flank multiple β-strands (Melcher, 2000). Recent studies have proposed that mutating the D residue in the LxD/N_{50-70}G motif in the 30K CCD can be used to functionally validate that a MP belongs to the 30K superfamily (Mushegian and Elena, 2015; Yu et al., 2013).

Plant-infecting rhabdoviruses (genera *Cytorhabdovirus* and *Nucleorhabdovirus*) unlike their animal- and human-infecting counterparts, are also thought to encode MP, some of which have been predicted to be 30K-like based on similar secondary structure to that of known members of the 30K-like superfamily (Dietzgen et al., 2006; Huang et al., 2005; Melcher, 2000). The rhabdoviral 30K-like MP superfamily candidates predicted by secondary structure are sonchus yellow net virus (SYNV) sc4 and lettuce necrotic yellows virus (LNYV) 4b (Dietzgen et al., 2006; Jackson et al., 2005; Melcher, 2000). LNYV 4b also showed limited amino acid sequence similarities with 30K MP superfamily members, capilloviruses and trichoviruses of the *Betaflexiviridae* family (Dietzgen et al., 2006). In addition, plant rhabdovirus putative MP genes have also been predicted by genome location. This is mostly as the third gene from the 3′ end of the genome between the phosphoprotein (P) and matrix protein (M) genes as

* Corresponding author. Tel.: +61 7 3346 6503; Fax: +61 7 3346 6501.
E-mail address: r.dietzgen@uq.edu.au (R.G. Dietzgen).
[1] Present address: IPAVE-CIAP-INTA, Av. 11 de Septiembre 4755, Cordoba 5020, Argentina.

http://dx.doi.org/10.1016/j.virol.2015.11.028
0042-6822/

for example, alfalfa dwarf virus (ADV) P3, lettuce yellow mottle virus (LYMoV) P3, maize mosaic virus (MMV) P3, maize Iranian mosaic virus P3, maize fine streak virus (MFSV) P4, rice yellow stunt virus (RYSV) P3, potato yellow dwarf virus (PYDV) Y protein, northern cereal mosaic virus (NCMV) P3, and taro vein chlorosis virus (TaVCV) P3 (Bandyopadhyay et al., 2010; Bejerman et al., 2015; Heim et al., 2008; Hiraguri et al., 2010; Huang et al., 2005; Massah et al., 2008; Reed et al., 2005; Revill et al., 2005; Scholthof et al., 1994; Tanno et al., 2000; Tsai et al., 2005). However, to date MP function has been experimentally demonstrated for P3 of only a single plant rhabdovirus. The nucleorhabdovirus RYSV P3 was shown to *trans*-complement the movement function of a movement-defective potato virus X (PVX) in *Nicotiana benthamiana* (Huang et al., 2005). Similarly, P3 of rice transitory yellowing virus (RTYV), a strain of RYSV, was also shown to function as MP (Hiraguri et al., 2012). Indirect evidence supporting a role for plant rhabdovirus P3 in cell-to-cell movement has been provided by autofluorescent protein fusions of SYNV sc4, PYDV Y, MFSV P4, ADV P3, and LNYV 4b which all localized to the cell periphery (Bandyopadhyay et al., 2010; Bejerman et al., 2015; Dietzgen et al., 2012; Goodin et al., 2007b; Tsai et al., 2005). A more in-depth investigation proposed a model for nucleorhabdovirus SYNV cell-to-cell movement and showed that two predominantly microtubule-associated *N. benthamiana* proteins, sc4 interactor protein 17 (sc4i17; motor kinesin homolog) and sc4i21 (*Arabidopsis thaliana* vascular one-zinc finger protein 1 homolog; AtVOZ1) (Mitsuda et al., 2004) interact with SYNV sc4 protein in a multi-protein complex that may aid cell-to-cell movement (Min et al., 2010). Using the first reverse genetics system for a plant negative-strand RNA virus, researchers have shown recently that sc4 protein is required for SYNV cell-to-cell movement (Wang et al., 2015).

Cell-to-cell movement function of a viral protein is typically tested by co-expressing a putative MP in *trans* with a movement-defective virus. In this assay, the movement-defective virus construct encodes green fluorescent protein (GFP), which permits a visual evaluation of cell-to-cell spread (Agranovsky et al., 1998; Ajjikuttira et al., 2005; Huang et al., 2005; Lauber et al., 1998; Lewandowski and Adkins, 2005; Li et al., 2004; Morozov et al., 1997; Ryabov et al., 1998; Solovyev et al., 1996; Zhang et al., 2005). Experimental validation of putative MP function has frequently employed tobamovirus- or PVX-based movement complementation systems (Hiraguri et al., 2012; Ishikawa et al., 2013; Niehl et al., 2014; Yu et al., 2013) and 30K-like MP have been shown to work in both (Lauber et al., 1998; Solovyev et al., 1996; Ziegler-Graff et al., 1991).

In this study, we tested movement function of two cytorhabdovirus putative MP using a movement-defective version of a turnip vein-clearing tobamovirus (TVCV) pro-vector system (Giritch et al., 2006). The tobamovirus pro-vector system was originally developed for commercial scale expression of a gene/protein of interest in plants using a modified TVCV vector that had been engineered for high-level replication by introducing multiple introns to make it more "plant-like" (Marillonnet et al., 2005). This pro-vector system is delivered by agroinfiltration into *N. benthamiana* leaves as a mixture consisting of three individual viral gene modules that assemble *in planta* to form a single infectious viral replicon (Giritch et al., 2006; Marillonnet et al., 2004). The three modules are: i) 5′ module encoding TVCV RNA-dependent RNA polymerase and TVCV P30 MP (pICH-17388), ii) 3′ module encoding GFP reporter and carrying a crucifer-infecting TMV 3′ NTR (pICH-7410) and iii) integrase module that combines the 5′ and 3′ modules into a single replicon through phiC31-dependent homologous recombination (pICH-14011). In the pICH-7410 module, the viral capsid protein was replaced by GFP rendering the replicon incapable of systemic spread but still maintaining efficient replication and cell-to-cell movement, which is indirectly visualized by GFP expression (Giritch et al., 2006).

Functional MP studies have yet to be conducted for any cytorhabdovirus. To continue our characterization of cytorhabdovirus-encoded proteins (Bejerman et al., 2015; Mann et al., 2015; Martin et al., 2012), we set out to experimentally validate the predicted cell-to-cell movement function of P3 of the cytorhabdoviruses, LNYV and ADV. Both viruses have a similar conserved 3′→5′ basic genome organization, nucleoprotein (N) – P – P3 – M – glycoprotein (G) – polymerase (L). However, ADV encodes an additional P6 ORF between G and L genes (Bejerman et al., 2015), similar to strawberry crinkle cytorhabdovirus (Mann and Dietzgen, 2014; Schoen et al., 2004). The predicted MP ORF for LNYV and ADV is at genome position 3 between P and M genes (referred to as P3). However, LNYV putative MP has been historically referred to as "4b", based on the relative size of the respective viral mRNA in northern blots (Dietzgen et al., 1989). We will refer here to both cytorhabdoviral MP as "P3". In this study, we demonstrate that LNYV P3 and ADV P3 function as MP by supporting the movement of a P30-defective TVCV replicon in *trans*. We also perform mutation analysis of the crucial 30K-like LxD/N_{50-70}G motif that is present in both of these MP and examine P3 interaction with a microtubule-associated host protein to provide further insights into the cell-to-cell movement process of these 30K-like MP.

Results

Comparison of putative plant rhabdovirus movement protein sequences with those of confirmed 30K-like MP superfamily members

Secondary structure predictions for putative MP of some plant rhabdoviruses, including LNYV P3, have revealed 30K-like MP sequence features (Melcher, 2000; Walker et al., 2011). To explore this in more detail we conducted sequence homology analyses for both LNYV P3 and the previously uncharacterized ADV P3 using the National Center for Biotechnology Information non-redundant database. BlastP searches identified a 30K-like MP domain in LNYV P3 between amino acids 40 and 185, but no such domain was found in ADV P3 sequence.

We next investigated whether LNYV P3 and ADV P3 shared any secondary structure homology with 30K superfamily tobamovirus members TMV and TVCV. Alignments based on both sequence and secondary structure similarities were carried out using PROMALS3D (Pei and Grishin, 2014). With respect to the 30K-specific CCD, both LNYV P3 and ADV P3 possessed a secondary structure pattern similar to that reported for members of the 30K superfamily. The consensus pattern of the CCD for 30K MP members consists of four α-helices (αA–αD) interspersed by seven β-elements (β1–β7) (Fig. 1A) (Melcher, 2000). However, for the cytorhabdovirus P3's, an additional β-element was observed after β7, named β7′ (Fig. 1A). Two of the conserved residues in the CCD, namely aspartic acid (D) and glycine (G) (Fig. 1A; black boxes) in the cytorhabdovirus P3 conform to the 30K-specific LxD/N_{50-70}G motif. This motif which starts at the end of the β2 sheet in what is called the 30K domain (Fig. 1A; second black box), is conserved for most 30K MP members (Melcher, 2000) and mutation of the D residue has been shown to cause the disruption of both, movement function and localization to PD for several 30K members (Bertens et al., 2000; Li et al., 2009; Yu et al., 2013; Zhang et al., 2012). An additional PROMALS3D alignment to test whether this motif is present in other plant rhabdovirus P3 sequences found that all available P3 protein sequences of cytorhabdoviruses (ADV, barley yellow striate mosaic virus, LNYV, LYMoV, persimmon virus A and NCMV) contained the D residue of the LxD/N_{50-70}G motif, whereas dichorhaviruses (orchid fleck virus and coffee ringspot

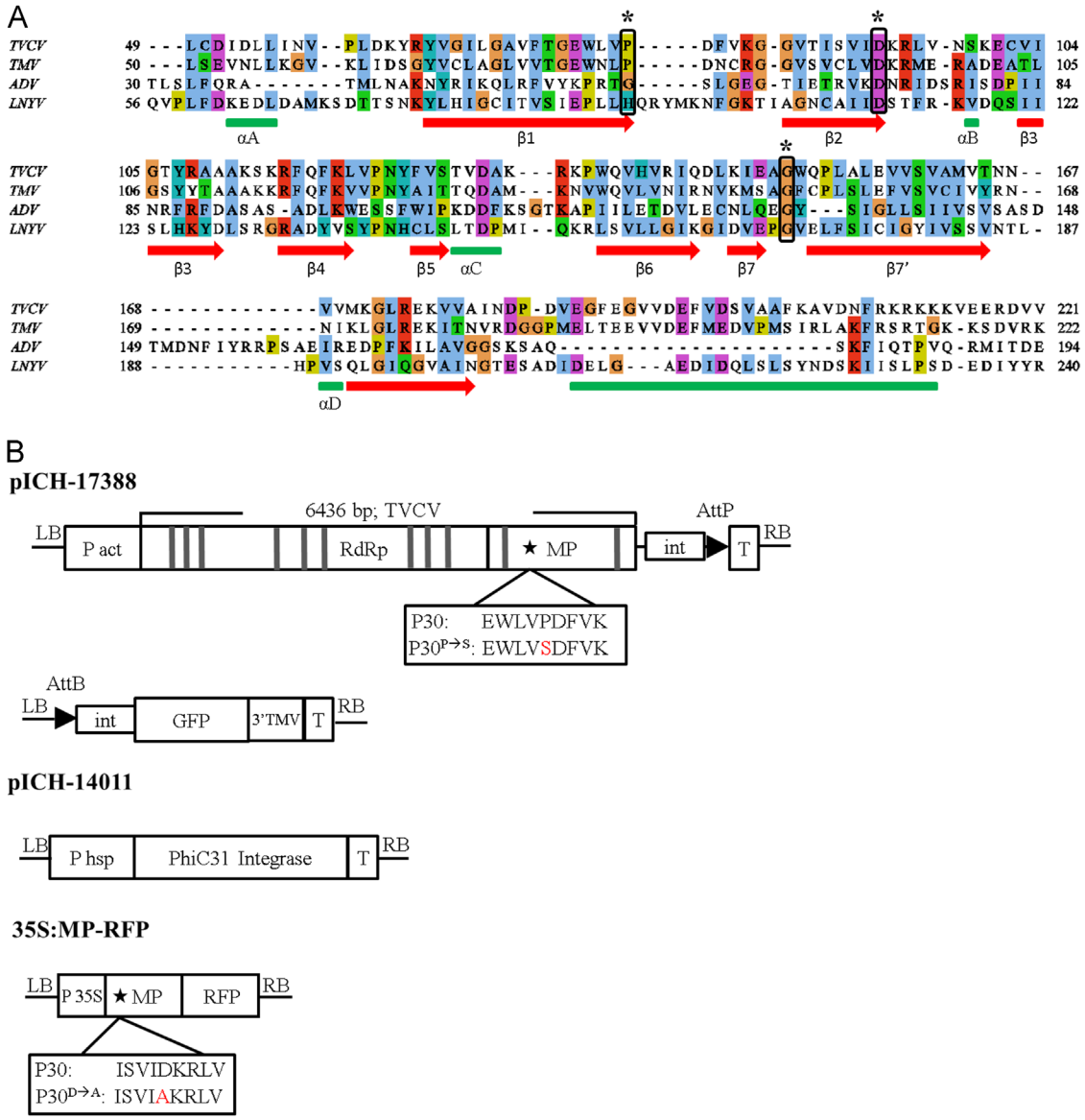

Fig. 1. Alignment of cytorhabdovirus and tobamovirus partial movement protein (MP) amino acid sequences and schematic diagrams of constructs used for movement *trans*-complementation. (A) PROMALS3D alignment depicting the 30K MP "common core" domain (Melcher, 2000) along with the secondary structure consensus denoted by α-helices (green bars) and β-elements (red arrows) below the alignment. TMV: tobacco mosaic virus (GenBank accession number NC_001367.1); TVCV: turnip vein-clearing virus (U03387.1); ADV: alfalfa dwarf virus (KP205452); LNYV: lettuce necrotic yellows virus (AJ867584.2). Black boxes with asterisks highlight key movement-related amino acid residues analyzed in this study. (B) Diagrams of movement pro-vector constructs. pICH-17388: TVCV RNA-dependent RNA polymerase (RdRp) and TVCV P30 MP; pICH-7410: GFP reporter and TMV 3′ non-translated region; pICH-14011: integrase module; P act: *Arabidopsis* actin 2 promoter; AttB and AttP (arrowheads): recombination sites; int and gray vertical bars: intron(s); star symbol: location of introduced mutation in the MP region of piCH17388 and 35S:MP-RFP; P hsp: *Arabidopsis* heat shock protein 81.1 promoter; RB/LB: T-DNA right/left border; P 35S: cauliflower mosaic virus promoter; T: nos terminator. *Trans*-complementing 35S:MP-RFP constructs were expressed from pSITE-4NB expression vector.

virus) (Dietzgen et al., 2014) have an N residue in this position (Supplementary Table 1). In contrast, a D or N residue in this position did not occur in putative MP of any nucleorhabdoviruses analyzed (datura yellow vein virus, eggplant mottle dwarf virus, maize mosaic virus, maize fine streak virus, maize Iranian mosaic virus, potato yellow dwarf virus, rice yellow stunt virus, and taro vein chlorosis virus) with the notable exception of sonchus yellow net virus, which features an N residue (Supplementary Table 1). Taken together, this data indicates that cytorhabdovirus P3 of LNYV and ADV are potential 30K-like MP members, with ADV P3 more diverged than LNYV based on BlastP searches.

TVCV pro-vector cell-to-cell movement complementation system

To test cell-to-cell movement complementation by cytorhabdovirus putative MP, we generated a movement-defective version of the previously described GFP-expressing TVCV pro-vector system (Marillonnet et al., 2004) (Fig. 1B). To ensure that the TVCV pro-vector system was working as expected, we agroinfiltrated *N. benthamiana* leaves with one, two or all three pro-vector modules (Fig. 1B) and monitored GFP expression to assess replication and cell-to-cell movement efficiency (data not shown). Confocal microscopic analysis showed significant cell-to-cell movement in *N. benthamiana* epidermal leaf cells only when all three modules, henceforth collectively referred to as "TVCV", were co-expressed. TVCV cell-to-cell spread appeared as large clusters of interconnected GFP-expressing cells as early as 3 days postinfiltration (dpi) (data not shown) but showed peak cell-to-cell spread by 7 dpi (Fig. 2, panel A).

To engineer a movement-deficient TVCV (denoted TVCVΔMP), a point mutation was introduced into the P30 MP gene of pICH-

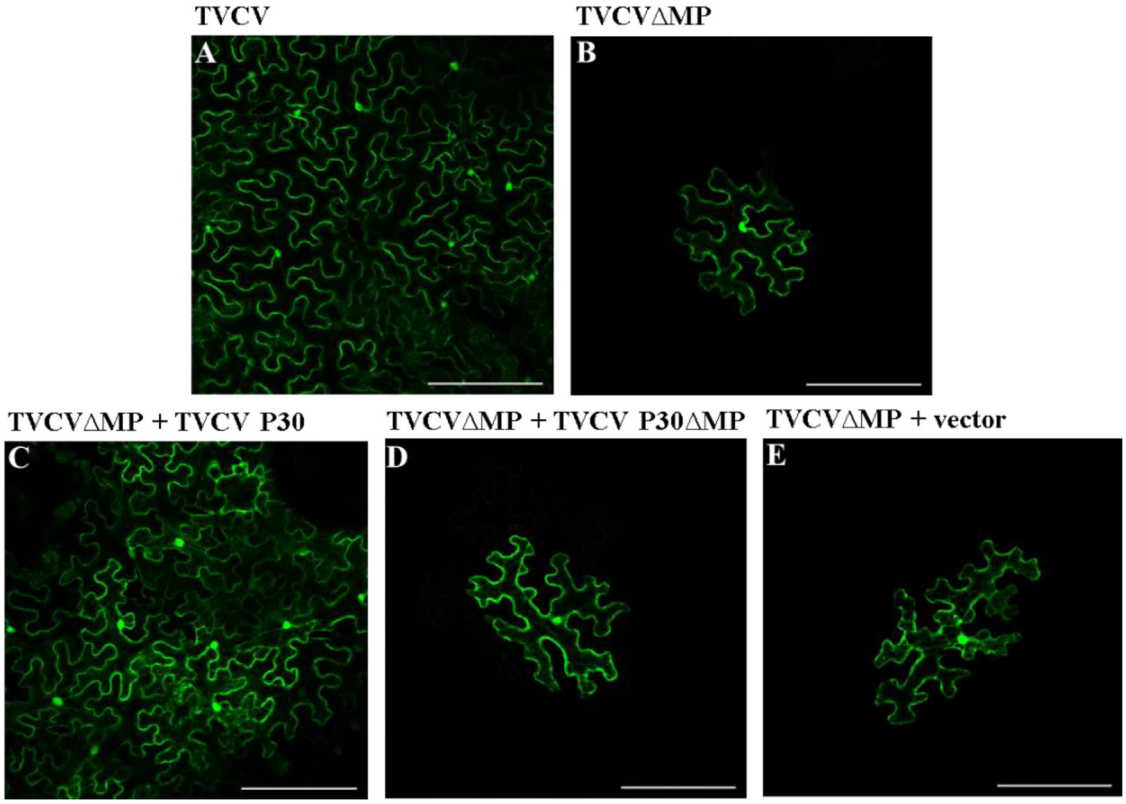

Fig. 2. Confocal microscope images of *N. benthamiana* leaves agroinfiltrated with a combination of TVCV pro-vector modules. (A) Co-expression of all three "wild-type" pro-vector modules [composed of pICH-17388 + pICH-7410 + pICH-14011 (collectively referred to as TVCV)]. Movement defective TVCV (TVCVΔMP) [composed of pICH-17388* (MP mutated) + pICH-7410 + pICH-14011] (B) plus either TVCV P30 (C), TVCV P30ΔMP (D) or empty (unfused RFP) vector (E). Agrobacterium solutions of TVCV modules were diluted to OD_{600} 0.015, while those carrying MP constructs were diluted to OD_{600} 0.0015. Live cell images were taken 7 days post agroinfiltration using a confocal microscope at 10 × magnification. Bars, 50 μm.

17388 leading to the replacement of proline at amino acid position 80 with serine (Fig. 1A, see first black box and Fig. 1B). This residue is typically located after or at the end of the β1 sheet in the 30K CCD (Fig. 1A) and its mutation had been shown to disrupt TMV movement (Deom and He, 1997) but to our knowledge this has yet to be confirmed for TVCV P30. To ensure cell-to-cell movement of TVCV could be clearly distinguished from that of TVCVΔMP following agroinfiltration of *N. benthamiana*, suspensions of agrobacteria carrying all three TVCV modules were diluted to a final OD_{600} of 0.015, which was sufficient to produce predominantly single fluorescing cells. Movement complementation was scored based on the number of GFP-expressing cells, whereby five or more adjoining cells (referred to as a large cluster) were considered as authentic cell-to-cell movement based on previous reports (Hiraguri et al., 2012; Yu et al., 2013). At 7 dpi, confocal microscope analysis of leaves agroinfiltrated with TVCVΔMP showed that GFP fluorescence was predominantly confined to single isolated epidermal cells (Fig. 2B). In contrast, TVCV encoding a functional P30 showed large clusters of GFP-expressing cells (Fig. 2A). TVCVΔMP did not show any spread of GFP fluorescence up to at least 12 dpi (data not shown). Taken together, this data shows that TVCVΔMP remained competent for replication, but lacked cell-to-cell movement since GFP fluorescence did not spread beyond initially infected cells into neighboring cells (Fig. 2B). This data also validates that the previously reported disruption of the TMV P30 movement function by a single P→S point mutation (Deom and He, 1997) has a similar effect when applied to TVCV P30.

To test if TVCVΔMP could be complemented in *trans*, a functional TVCV P30-red fluorescent protein (RFP) fusion construct (OD_{600} = 0.0015) was co-agroinfiltrated with TVCVΔMP into *N. benthamiana* leaves. The RFP fluorescent tag was used as a marker for MP expression during movement complementation assays (Supplementary Fig. 1). At 7 dpi, leaves agroinfiltrated with TVCVΔMP showed large clusters of GFP-expressing cells only when co-expressed with TVCV P30-RFP (Fig. 2, panel C and Supplementary Fig. 1A, top row), but not with TVCV P30ΔMP-RFP (D→A mutation in the LxD/N_{50-70}G motif) (Fig. 2, panel D and Supplementary Fig. 1B, top row) or unfused RFP ("vector") (Fig. 2, panel E and Supplementary Fig. 1C, bottom row). Cell-to-cell movement complementation of TVCVΔMP by TVCV P30-RFP was observed as early as 5 dpi (data not shown) which was 2 days delayed in comparison to "wild-type" TVCV which first showed replicon spread at 3 dpi (data not shown). We tested RFP fusions to both the N- and C-terminus of TVCV P30 for movement *trans*-complementation; however only fusions to the C-terminus were successful (data not shown). This indicates that TVCV P30 like other 30K MP only maintain cell-to-cell movement activity when a tag is fused to their C-terminus, whereas N-terminal fusions are non-functional (Yu et al., 2013).

Cytorhabdovirus P3 proteins trans-complement movement-deficient TVCV

The validated TVCVΔMP movement complementation system (Figs. 1B and 2) was used to determine whether transient expression of cytorhabdovirus P3-RFP constructs could facilitate cell-to-cell movement of movement-deficient TVCVΔMP. Similar to the ectopically expressed TVCV P30-RFP positive control (Fig. 2, panel C), the RFP tag was also fused to the C-terminus of the cytorhabdovirus P3 proteins being tested. Transient expression of all MP-RFP fusion proteins was confirmed during movement

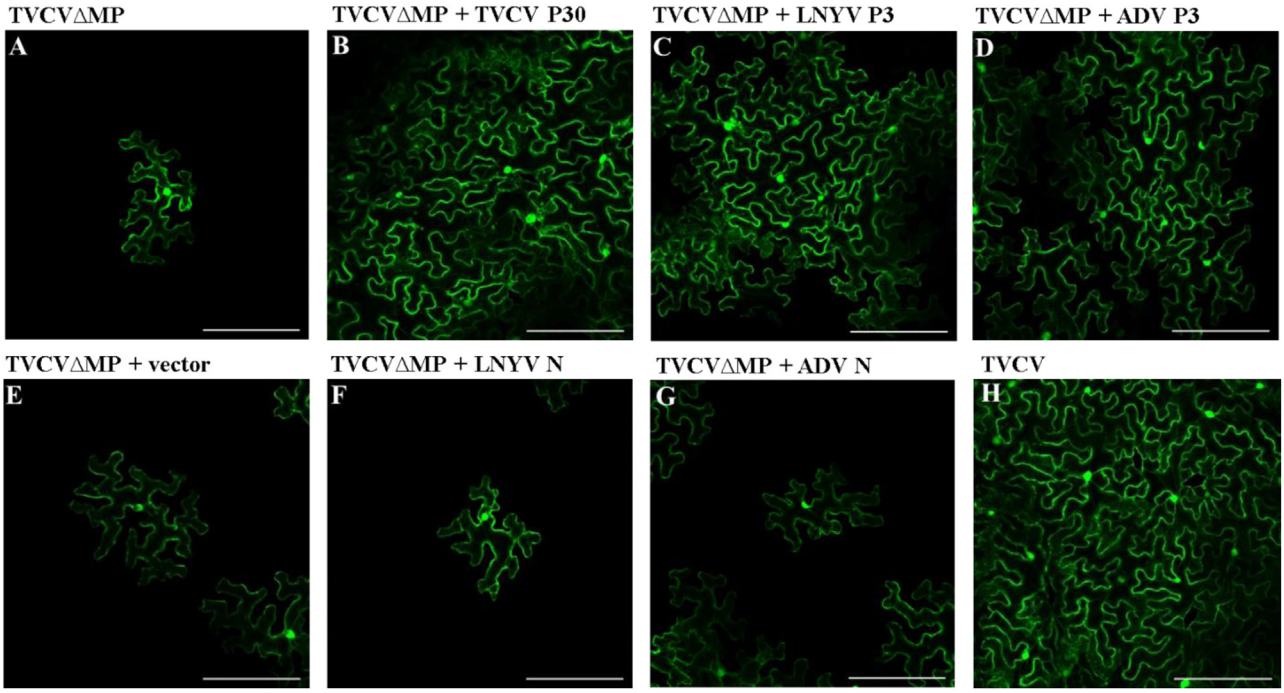

Fig. 3. *Trans*-complementation movement assay of cytorhabdovirus P3 proteins. *N. benthamiana* leaves were agroinfiltrated with TVCVΔMP [composed of pICH-17388* (MP mutated)+pICH-7410+pICH-14011] (A) plus either TVCV P30 (B), LNYV P3 (C), ADV P3 (D), empty (unfused RFP) vector (E), LNYV N (F), or ADV N (G). Agrobacterium solutions of TVCV modules were diluted to OD_{600} 0.015 while those carrying MP constructs were diluted to OD_{600} 0.0015. Live cell images were taken at 7 dpi using a confocal microscope at 10 × magnification. Bars, 50 μm. TVCV (H): co-expression of all three "wild-type" pro-vector modules.

Table 1
Cell-to-cell movement *trans*-complementation results for cytorhabdovirus P3 and TVCV P30.

TVCVΔMP+	dpi	1–2 cells	3–4 cells	≥5 cells	[a]Total foci counted	Virus movement efficiency (%) (5 or more cells)
TVCV P30-RFP	5	9	2	24	35	69
	7	15	7	55	77	71
LNYV P3-RFP	5	42	15	13	70	19
	7	72	28	58	158	37
ADV P3-RFP	5	55	8	5	68	7
	7	95	15	21	131	16
LNYV N-RFP	5	47	3	0	50	0
	7	87	3	0	90	0
ADV N-RFP	5	41	4	3	48	6
	7	75	13	1	89	1
Vector	5	54	5	0	59	0
	7	78	10	0	88	0

dpi; days post infiltration; TVCVΔMP: movement defective TVCV; Vector: unfused RFP vector control.

[a] Foci were counted using four individual biological replicates.

complementation assays by confocal microscopy (Supplementary Fig. 1A and C). At 7 dpi, TVCVΔMP co-expressed with LNYV P3-RFP or ADV P3-RFP showed large clusters of GFP-expressing cells similar to TVCV P30 (Fig. 3 panels B–D and Supplementary Fig. 1A). On the other hand, when TVCVΔMP was co-expressed with unfused RFP ("vector") or with cytorhabdovirus nucleoprotein (N)-RFP, only single cells expressed GFP (Fig. 3, panels E–G and Supplementary Fig. 1C). We measured the efficiency of cell-to-cell movement complementation by counting the number of cells expressing GFP at both 5 and 7 dpi (Table 1). Cell clusters showing GFP expression in five or more cells were tallied and then divided by the total number of examined cells to estimate movement efficiency. Movement complementation efficiency approached nil at 7 dpi when TVCVΔMP was co-expressed with unfused RFP, LNYV N-RFP or ADV N-RFP (Table 1). In contrast, TVCVΔMP cell-to-cell movement complementation by LNYV P3-RFP had 19% efficiency at 5 dpi, which increased to 37% at 7 dpi. ADV P3-RFP showed 7% efficiency at 5 dpi, which increased to 16% at 7 dpi. Expression of either P3 facilitated increased movement from 5 to 7 dpi, but LNYV P3 was more than twice as efficient at *trans*-complementing TVCVΔMP cell-to-cell movement than ADV P3 (Table 1). However, TVCV P30-RFP was most efficient with approximately 70% at both 5 and 7 dpi (Table 1). Although TVCV P30-RFP showed greater compatibility with TVCVΔMP, nearly 30% of observed cells did not show efficient cell-to-cell movement complementation. However, this was not the case for the "wild-type" TVCV, which showed 100% cell-to-cell spread in agroinfiltrated patches (Fig. 3, panel H). This result may indicate that delivery by agroinfiltration of all four individual constructs (i.e., the three TMV modules plus the *trans*-complementing MP) together into the same *N. benthamiana* leaf cells was not always successful. Taken together, this data provides evidence that LNYV P3 and ADV P3 function as cell-to-cell MP.

Mutation of a conserved residue in 30K domain abolishes cytorhabdovirus P3 movement function and effects LNYV P3 subcellular localization

Cytorhabdovirus P3 sequence analysis (Fig. 1A and Supplementary Table 1) and tobamovirus movement *trans*-complementation data (Fig. 3) provide evidence that P3 of both cytorhabdoviruses are 30K-like MP. Like TVCV P30, both LNYV P3 and ADV P3 amino acid sequences contain the D residue of the $LxD/N_{50-70}G$ motif. We therefore examined the impact on P3 movement activity and intracellular localization when this aspartic acid residue was replaced with alanine (D→A). Expression of mutated P3ΔMP-RFP fusion constructs during movement complementation assays was confirmed by confocal microscopy (Supplementary Fig. 1B). At 7 dpi, leaves agroinfiltrated with TVCVΔMP showed GFP expression only in single cells (Fig. 3, panel

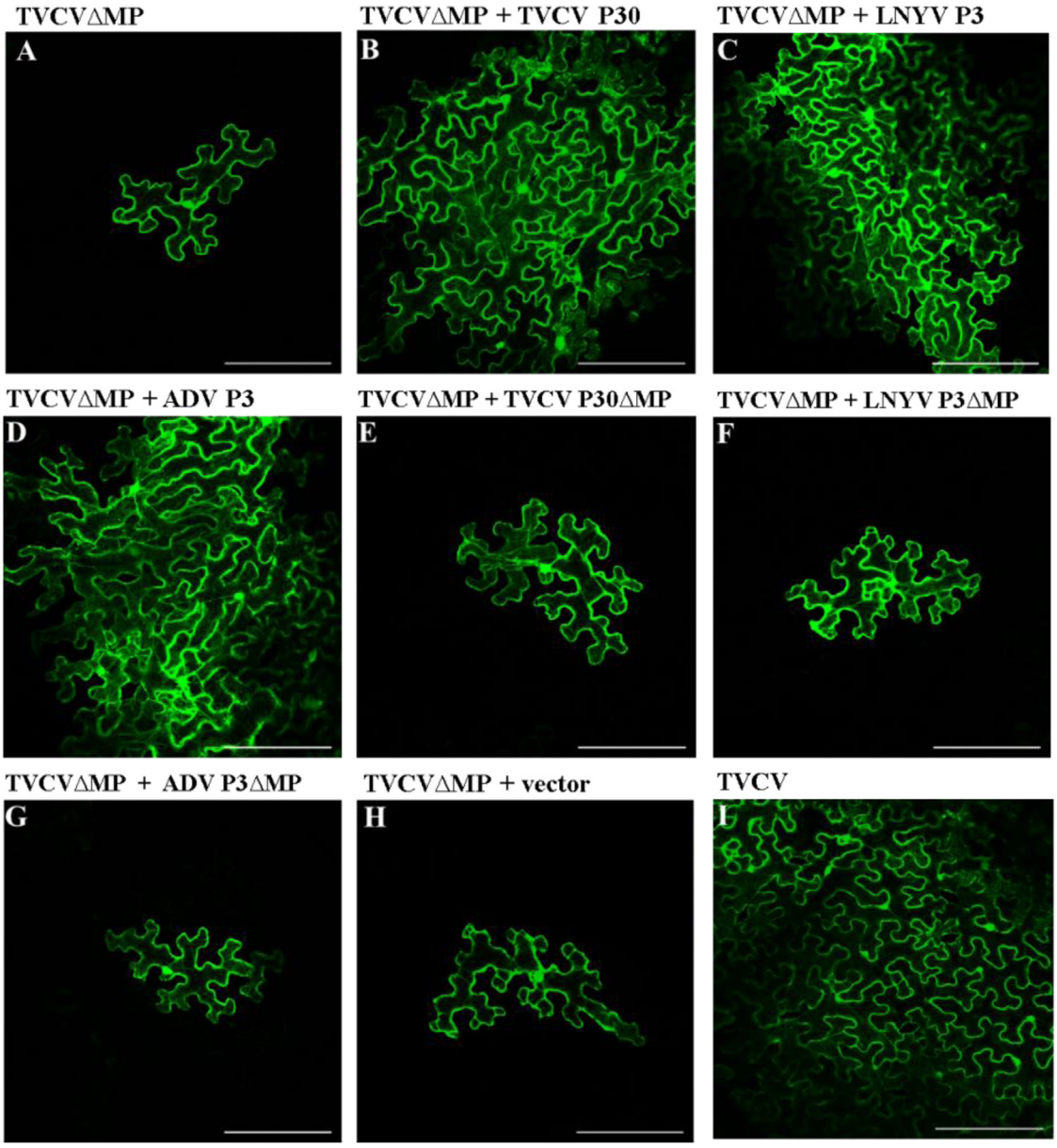

Fig. 4. *Trans*-complementation movement assay of mutant cytorhabdovirus P3 proteins. *N. benthamiana* leaves were agroinfiltrated with TVCVΔMP [composed of pICH-17388* (MP mutated)+pICH-7410+pICH-14011] (A) plus either functional MP (TVCV P30, LNYV P3, and ADV P3) (B–D) or mutated MP (TVCV P30ΔMP, LNYV P3ΔMP, and ADV P3ΔMP) (E–G) or unfused RFP vector (H). Agrobacterium solutions of TVCV modules were diluted to OD_{600} 0.015 while those carrying MP constructs were diluted to OD_{600} 0.0015. Live cell images were taken at 7 dpi using a confocal microscope at 10 × magnification. Bars, 50 μm. TVCV (I): co-expression of all three "wild-type" pro-vector modules.

A and Fig. 4, panel A), whereas large clusters of GFP-expressing cells were seen when TVCVΔMP was co-expressed with the functional MP, TVCV P30-RFP, LNYV P3-RFP and ADV P3-RFP (Fig. 4, panels B–D), as shown in our previous experiment (Fig. 3, panels B–D). In contrast, GFP fluorescence was predominantly confined to single isolated epidermal cells when TVCVΔMP was co-expressed with the mutated MP, TVCV P30-RFPΔMP, LNYV P3-RFPΔMP and ADV P3-RFPΔMP similar to the unfused RFP control ("vector") (Fig. 4, panels E–H and Supplementary Fig. 1B and C). This indicates that like for other 30K superfamily members that possess the $LxD/N_{50-70}G$ motif, mutation of the aspartic acid residue in LNYV P3 and ADV P3 interferes with the cell-to-cell movement activity of these proteins.

We also investigated if the D→A mutation in the $LxD/N_{50-70}G$ motif of cytorhabdovirus P3 had an effect on protein intracellular localization. Typically, viral MP including members of the 30K MP family localize to the cell periphery to facilitate cell-to-cell spread of nucleoprotein complexes through PD. *N. benthamiana* leaves agroinfiltrated with RFP fusions to functional and mutant (ΔMP) constructs showed detectable fluorescence in confocal microscopy using increased power settings (Supplementary Fig. 2A). However, GFP fusions generally showed stronger fluorescence than RFP fusions and the former were chosen to determine subcellular localization in relation to aniline blue fluorochrome, a callose-binding plasmodesmata marker dye. Expression of GFP fusions to either functional or dysfunctional MP was readily detectable by western blot using GFP monoclonal antibodies (Supplementary Fig. 2B). For easier visualization, GFP and aniline blue images were false-colored to yellow and cyan, respectively. At 2 dpi, *N. benthamiana* leaves agroinfiltrated with GFP fusions to TVCV P30, LNYV P3 and ADV P3 co-localized with or were in close proximity to the aniline blue marker on the cell periphery in 78–90% of foci

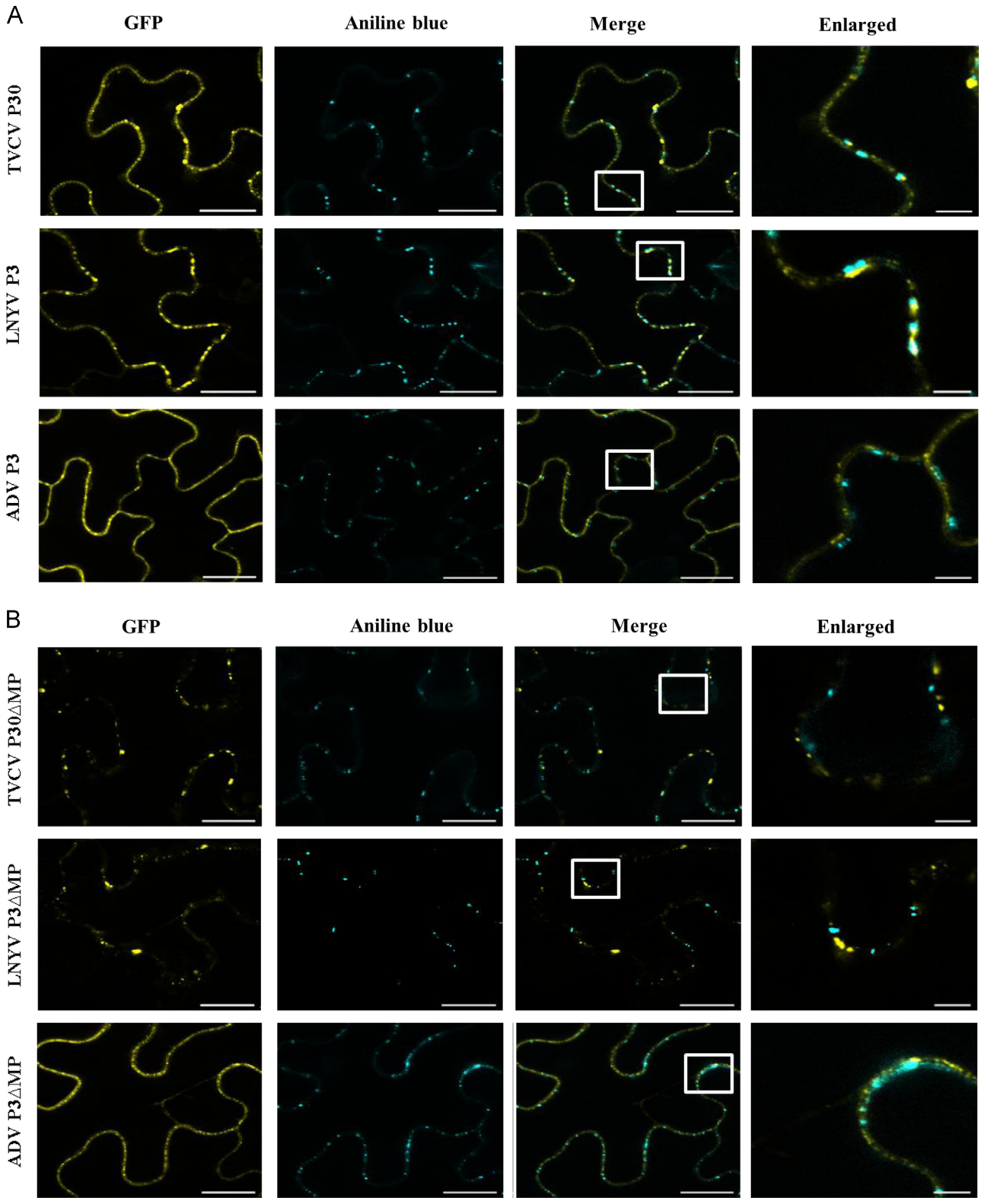

Fig. 5. Co-localization of cytorhabdovirus P3 and TVCV P30 with aniline blue fluorochrome. *N. benthamiana* leaves stained with the PD marker aniline blue, were agroinfiltrated with either GFP-fusions to functional MP (TVCV P30, LNYV P3, and ADV P3) (A) or mutated MP (TVCV P30ΔMP, LNYV P3ΔMP, and ADV P3ΔMP) (B). Magnified sections of images (right side of panels A and B) are highlighted with white boxes. For easier visualization, GFP and aniline blue fluorescent images were false colored to yellow and cyan, respectively. Live cell images were taken at 2 dpi using a confocal microscope at 40 × magnification. Bars, 20 μm.

analyzed (Fig. 5A and Supplementary Table 2). However, GFP fusions to TVCV P30ΔMP and LNYV P3ΔMP showed a 5- to 10-fold reduction in the co-localization with aniline blue foci and reduced accumulation along the cell periphery (Compare Fig. 5A and B; Supplementary Table 2). In contrast, the GFP fusion to ADV P3ΔMP co-localized with aniline blue at PD but showed a slightly more punctate distribution on the cell periphery than the functional ADV P3 (Fig. 5, compare A and B; Supplementary Table 2). To

validate these intracellular localization data, we also co-expressed functional and dysfunctional viral MP with *A. thaliana* plasmodesmata localized protein (PDLP) 1, which is known to localize within PD and to be involved in the movement process of some plant viruses (Amari et al., 2010). GFP-fusions to LNYV P3 and TVCV P30 showed many co-localizing aggregates on the cell periphery when co-expressed with PDLP1-RFP (Supplementary Fig. 3A). In contrast, GFP fusions to ADV P3 (Supplementary Fig. 3A) and all dysfunctional MP (Supplementary Fig. 3B) were distributed smoothly along the cell periphery showing no co-localizing aggregates when co-expressed with PDLP1-RFP. This is similar to the distribution observed for ADV P3 and all dysfunctional MP when expressed without PDLP1-RFP (Supplementary Fig. 3C). Bimolecular fluorescence complementation (BiFC) analysis did not detect any protein–protein interactions involving PDLP1 (data not shown). Taken together, this data confirms PD localization of the studied MP. It also appears to indicate that PDLP1 interaction may not be required by these MPs and that the D→A mutation in the 30K LxD/N_{50-70}G motif impairs PD targeting of LNYV P3 and TVCV P30.

LNYV P3 and TVCV P30 but not ADV P3 interact with the microtubule-associated transcriptional activator NbVOZ1

Previous reports have proposed that SYNV sc4, the P3 of this nucleorhabdovirus, is a 30K-like MP based on secondary structure predictions and intracellular localization to the cell periphery (Goodin et al., 2007b; Melcher, 2000; Min et al., 2010). One of those studies identified that SYNV sc4 interacted in yeast 2-hybrid and BiFC assays with two *N. benthamiana* proteins termed sc4 interactor protein 17 (sc4i17; motor kinesin homolog) and sc4i21 (*A. thaliana* vascular one-zinc finger protein 1 homolog) (Min et al., 2010). These microtubule-associated proteins were implicated in SYNV cell-to-cell movement (Min et al., 2010). We chose to study sc4i21, henceforth referred to as NbVOZ1, to determine if this microtubule-associated transcriptional activator protein also interacts with 30K-like MP of other viruses, in particular TVCV P30, LNYV P3 and ADV P3. NbVOZ1 gene was PCR-amplified from total *N. benthamiana* RNA, cloned into pDONR221, sequenced, recombined into pSITE-RFP-N1 and transiently expressed following agroinfiltration. At 2 dpi, confocal microscope analysis of agroinfiltrated *N. benthamiana* leaves showed that NbVOZ1-RFP accumulated uniformly on microtubules and in small aggregates on the cell periphery (Fig. 6C) as previously shown (Min et al., 2010). When NbVOZ1-RFP was co-expressed with viral MP-GFP, large cytosolic or cell periphery co-localizing aggregates were seen with TVCV P30-GFP and LNYV P3-GFP (Fig. 6A). No such aggregates were observed for either of these MP fusions when expressed individually (Fig. 6C). In contrast, NbVOZ1-RFP co-expression with ADV P3-GFP showed that both proteins uniformly accumulated on the cell periphery (Fig. 6A) similar to when ADV P3-GFP was expressed alone (Fig. 6C). Co-expression of NbVOZ1-RFP with dysfunctional TVCV P30ΔMP-GFP or LNYV P3ΔMP-GFP no longer showed the large co-localizing aggregates that were observed with the functional MP (Fig. 6; compare A and B). Instead NbVOZ1-RFP localized on microtubules and in small aggregates on the cell periphery similar to when this protein was expressed alone (Fig. 6C), suggesting that dysfunctional LNYV P3ΔMP and TVCV P30ΔMP did not co-localize with NbVOZ1. In contrast, NbVOZ1-RFP co-expression with ADV P3ΔMP-GFP showed a uniform to punctate accumulation on the cell periphery (Fig. 6B) similar to when ADV P3ΔMP-GFP was expressed alone (Fig. 6C).

The data above suggest that LNYV P3 and TVCV P30, but apparently not ADV P3, may utilize NbVOZ1 to aid virus movement. To determine if the observed re-localization effect by LNYV P3 and TVCV P30 on NbVOZ1 subcellular distribution involves heterotypic protein–protein interactions, BiFC assay was done in all pairwise combinations using Glutathione-S-transferase (GST) as a non-binding control. In agroinfiltrated transgenic *N. benthamiana* cells expressing CFP-histone 2B nuclear marker, TVCV

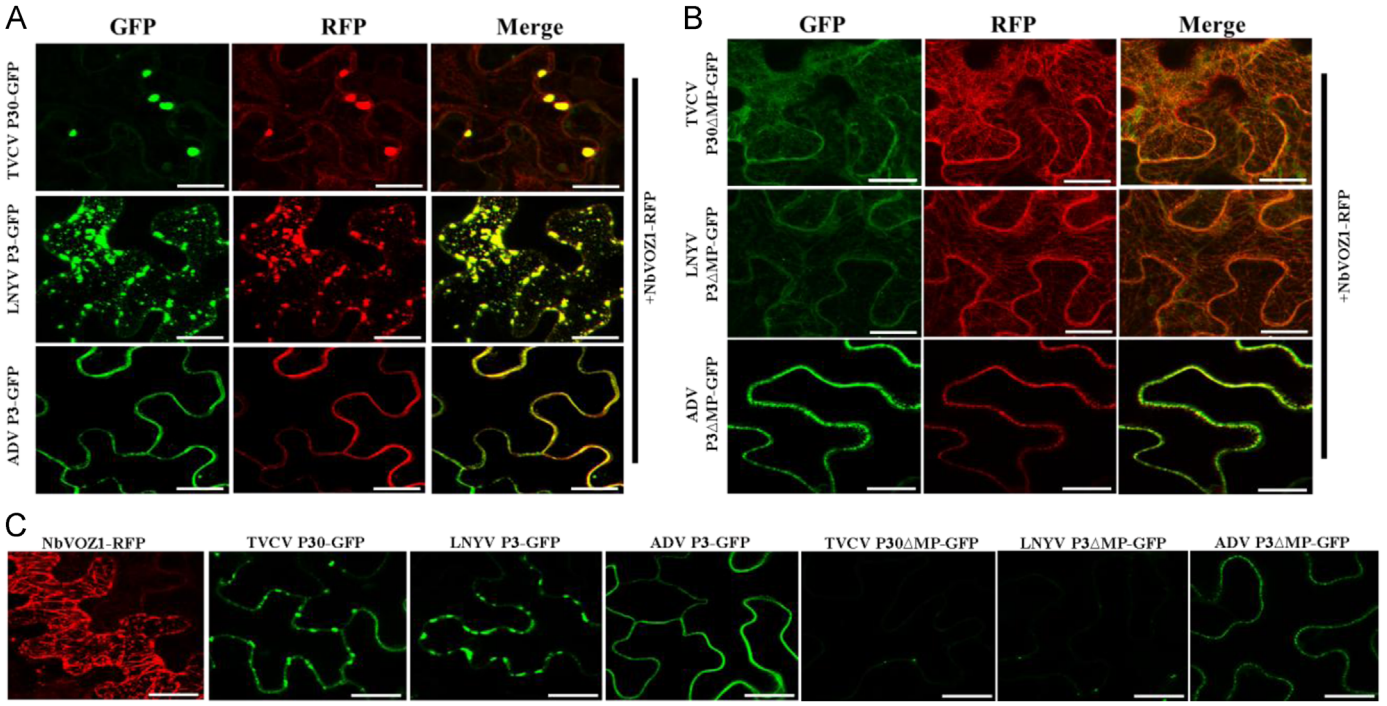

Fig. 6. Transient co-expression of cytorhabdovirus P3 or TVCV P30 and microtubule-associated NbVOZ1. *N. benthamiana* leaves were agroinfiltrated with constructs encoding NbVOZ1-RFP plus GFP-fusions to either functional MP (TVCV P30, LNYV P3, and ADV P3) (A) or mutated MP (TVCV P30ΔMP, LNYV P3ΔMP, and ADV P3ΔMP) (B). Controls for the individual protein expression of MP or ΔMP and NbVOZ1 fused to GFP or RFP, respectively (C) are shown below co-expression panels (A, B). Live cell z-stack images were taken at 2 dpi using a confocal microscope at 40 × magnification. Bars, 20 μm.

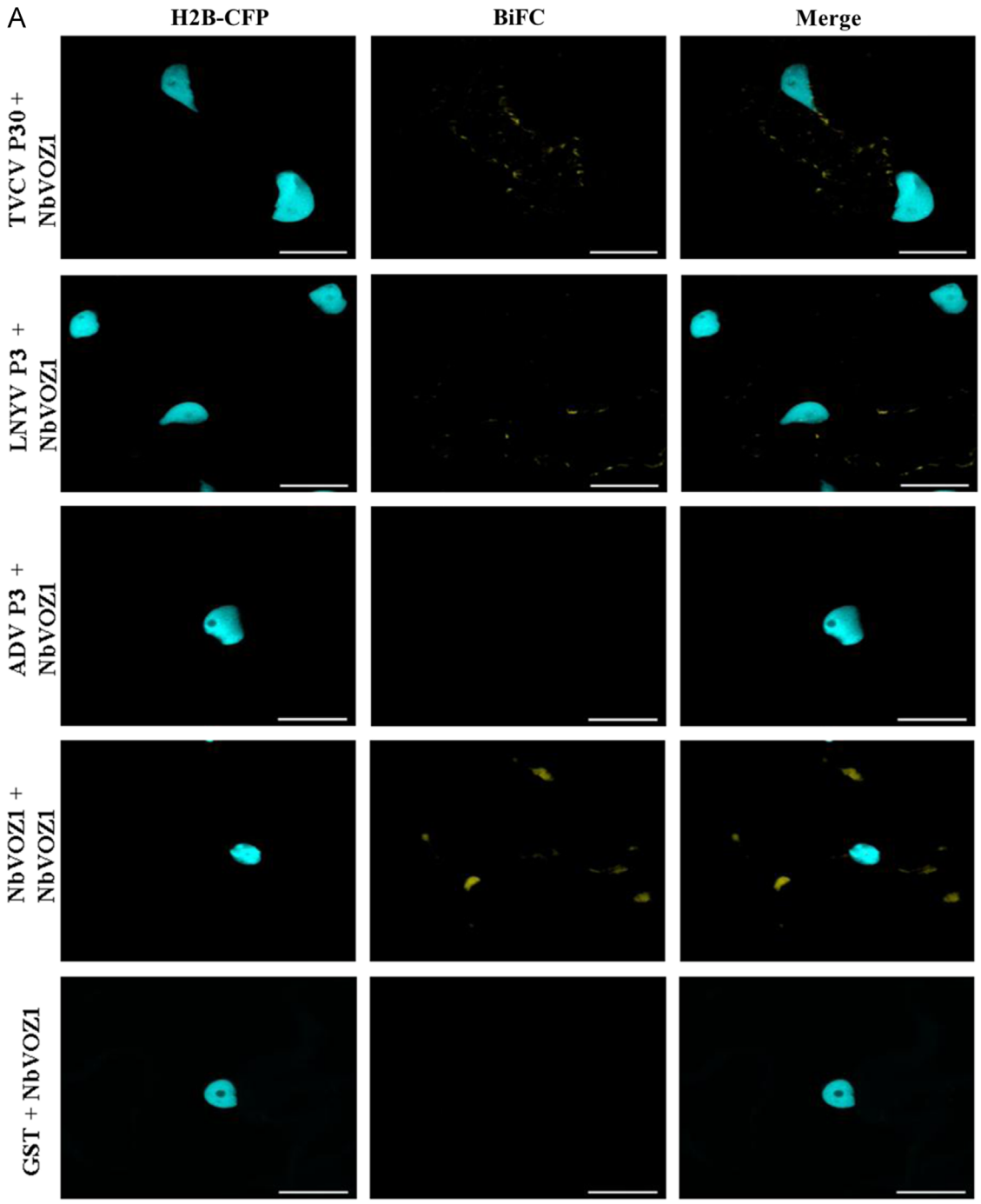

Fig. 7. Bimolecular fluorescence complementation assay of cytorhabdovirus P3 or TVCV P30 interactions with transcriptional activator NbVOZ1. Protein–protein interaction assays were carried out in transgenic *N. benthamiana* expressing CFP fused to the nuclear marker histone 2B (CFP-H2B). Transgenic plants were agroinfiltrated with NbVOZ1 plus either functional MP (TVCV P30, LNYV P3, and ADV P3) (A) or mutated MP (TVCV P30ΔMP, LNYV P3ΔMP, and ADV P3ΔMP) (B). Proteins listed first in the pair of interactors were expressed as fusions to the carboxy-terminal half of yellow fluorescent protein (YFP). Those listed second were expressed as fusions to the amino-terminal half of YFP. From left to right panel show H2B-CFP (nuclear localization), BiFC (YFP fluorescence) and merged images for each assayed pair of proteins. Glutathione-S-transferase (GST) was used as a non-binding control to validate interactions. Live cell z-stack images were taken at 2 dpi using a confocal microscope at 40 × magnification. Bars, 20 μm.

P30 and LNYV P3 showed an interaction with NbVOZ1 (Fig. 7A), whereas no interaction was detected for ADV P3 or any of the mutated MPs (TVCV P30ΔMP, LNYV P3ΔMP, and ADV P3ΔMP) (Fig. 7A and B). BiFC confirmed that NbVOZ1 was capable of self-interaction as shown previously (Min et al., 2010) and none of the tested proteins interacted with GST (Fig. 7B). Taken together, mutation of the D residue in the 30K-specific LxD/N_{50-70}G motif appears to disrupt movement complementation for all tested MP and interaction with NbVOZ1 specifically for TVCV P30 and LNYV P3 but not ADV P3. This suggests that TVCV P30 and LNYV P3 may utilize NbVOZ1 to aid virus cell-to-cell movement.

Discussion

Plant viral MP mediate the transport of viral genomes mostly as nucleoprotein complexes from an infected cell to adjacent uninfected cells via the PD (Lazarowitz and Beachy, 1999; Liu and

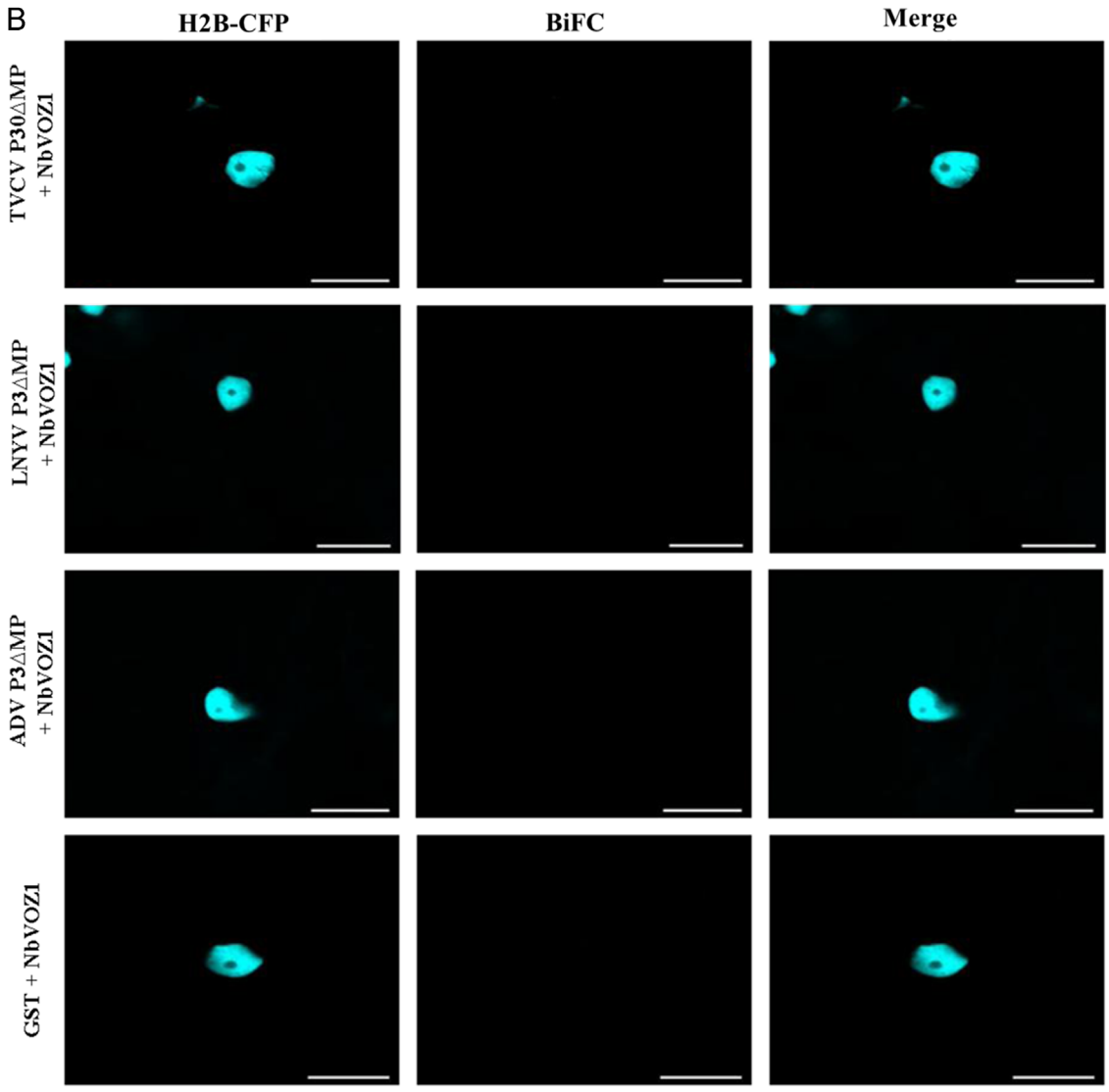

Fig. 7. (*continued*)

Nelson, 2013; Scholthof, 2005; Tilsner et al., 2014). This process also involves PD-localized host proteins and the plant cytoskeleton (Amari et al., 2010; Heinlein et al., 1998a; Niehl et al., 2014). Movement *trans*-complementation assays have provided the means to experimentally validate MP function (Ziegler-Graff et al., 1991). This approach is especially useful when studying proteins of viruses that lack reverse genetics systems. No infectious cDNA clones are currently available for LNYV and ADV to directly study functions of encoded proteins (Mann and Dietzgen, 2014), but such a system was recently developed for SYNV and demonstrated the MP function of its sc4 protein (Wang et al., 2015).

Here we show that P3 proteins of the cytorhabdoviruses LNYV and ADV *trans*-complemented a movement-defective TVCV replicon in *N. benthamiana*. LNYV P3 more efficiently supported TVCV movement than ADV P3 but neither had the same high efficiency as the homologous TVCV P30. This is the first study to functionally demonstrate that cytorhabdovirus P3 proteins act as cell-to-cell MP. This is also the first report demonstrating use of a modular TVCV pro-vector system to test movement function. We show that these cytorhabdovirus MP belong to the 30K-like superfamily of MP as predicted by *in silico* analyses (Dietzgen et al., 2006; Heim et al., 2008; Walker et al., 2011). We provide several lines of evidence to suggest LNYV P3 MP functions more like TVCV P30 MP than ADV P3. Like TVCV P30, LNYV P3 was 1) capable of *trans*-complementing TVCV movement, 2) significantly affected by a mutation in the 30K CCD LxD/N_{50-70}G motif and 3) interacted with the *N. benthamiana* microtubule-associated transcriptional activator NbVOZ1. Therefore, LNYV P3 and TVCV P30 may facilitate cell-to-cell movement using a similar mechanism, which may be aided by interaction with NbVOZ1, while ADV P3 may facilitate movement by an as yet unidentified mechanism that does not involve interaction with NbVOZ1.

It is not surprising that the P3 MP of the cytorhabdoviruses LNYV and ADV were capable of complementing TVCV movement (Fig. 3) given past complementation studies have shown that 30K-like MP can functionally replace the MP and support the cell-to-cell movement of related (Giesman-Cookmeyer et al., 1995; Mise et al., 1993) or unrelated viruses (Lauber et al., 1998; Morozov et al., 1997; Ryabov et al., 1998; Solovyev et al., 1996). However, this had not been shown previously for a cytorhabdovirus using a tobamovirus-based system. Our results confirm the functional homology typically observed for 30K-like MP (Giesman-Cookmeyer et al., 1995). However, the efficiency in *trans*-complementing the movement of TVCV by either LNYV P3 or ADV P3 was lower than the ectopically expressed “wild-type” TVCV P30 (Table 1). The lower efficiency may be due to intrinsic MP

differences between negative-sense cytorhabdoviruses and positive-sense tobamoviruses. MP of the 30K superfamily were shown to be more efficient at complementing the movement of related viruses (Niehl et al., 2014) than unrelated viruses (Tamai et al., 2003). Thus, although 30K-like MPs are capable of supporting the movement of unrelated viruses, the efficiency at which this occurs is likely lower than for related viruses as shown here for cytorhabdovirus MP versus TVCV MP. This is supported in the literature by numerous *trans*-complementation studies which show that the heterologous MP being tested was less efficient than the MP originally encoded by the movement-defective virus (Hiraguri et al., 2012; Huang et al., 2005; Ishikawa et al., 2013; Yu et al., 2013). Similar to our study which showed that LNYV P3 was ~2 times less efficient than the positive control MP at 7 dpi, RTYV P3 was found to be approximately ~1.5 times less efficient in *trans*-complementation activity as compared to the MP encoded by the movement-defective tobamovirus (Hiraguri et al., 2012).

It has been proposed that the conserved aspartic acid residue in the LxD/N_{50-70}G motif located in the β2 strand of 30K MPs may be a hallmark for the identification of candidate 30K family members (Mushegian and Elena, 2015; Yu et al., 2013). Mutation of this residue has been previously shown to cause both, a loss in movement function and PD localization for several 30K MP members including cauliflower mosaic virus P1, tomato spotted wilt virus NSm, raspberry leaf blotch virus P4, and rice stripe virus pc4 (Li et al., 2009; Thomas and Maule, 1995; Yu et al., 2013; Zhang et al., 2012). Our data support this identification scheme since both LNYV P3 and ADV P3 along with the positive control TVCV P30 lost movement complementation function after this D→A mutation was introduced (Fig. 4). However, this mutation generated differential results in our study with respect to intracellular localization (Fig. 5). Typically, MP localization at the PD is strongly correlated with cell-to-cell movement function (Sasaki et al., 2006; Tilsner et al., 2010; Yu et al., 2013). Although this appeared to be the case for LNYV P3ΔMP and TVCV P30ΔMP which showed a reduction in cell periphery accumulation and loss in PD localization similar to other reported 30K ΔMP (Bertens et al., 2000; Yu et al., 2013), ADV P3ΔMP localization was mostly unaffected (Fig. 5). Instead, ADV P3ΔMP cell periphery accumulation remained mostly unchanged and appeared to still target the PD (Fig. 5). This may suggest that PD localization and cell-to-cell movement function may not always be correlated. However, it is possible that the sequence for PD localization of ADV P3 may reside beyond the point mutation used in this study (for example within the β2 strand). This hypothesis is supported by studies which show that mutations in the β1 and β2 strands for some 30K MP did not always result in concurrent loss of movement function and PD localization (Kahn et al., 1998; Li et al., 2009; Yu et al., 2013; Zhang et al., 2012). Thus, although mutation of the conserved aspartic acid residue seems to broadly disrupt 30K movement, it does not appear to have the same effect on PD localization for some 30K-like MP such as ADV P3. This phenomenon may warrant further investigation.

Plant viral MP have been shown to interact with host cytoskeleton components such as actin filaments and microtubules to accomplish viral intracellular movement (Amari et al., 2011; Boyko et al., 2007; Cho et al., 2012; Harries et al., 2009; Niehl et al., 2014; Wright et al., 2010, 2007). The role of microtubules in viral cell-to-cell movement has been investigated for a small number of plant viruses including SYNV (Min et al., 2010) tomato mosaic virus (Padgett et al., 1996), potato mop-top virus (PMTV) (Wright et al., 2010), PVX (Cho et al., 2012), beet yellows virus (Karasev et al., 1992), grapevine fanleaf virus (Laporte et al., 2003) and mostly notably TMV (Niehl et al., 2013). TMV P30 MP directly binds to and interacts with microtubules (Boutant et al., 2009; Ferralli et al., 2006; Heinlein et al., 1998a) including tubulin (Ashby et al., 2006; Heinlein et al., 1998b), and disruption to the microtubule interaction inhibits TMV movement (Boyko et al., 2007). Here we show that both TVCV P30 and LNYV P3, but not ADV P3 co-localize and interact with the *N. benthamiana* microtubule-associated NbVOZ1 (Figs. 6 and 7), a host factor implicated in SYNV cell-to-cell movement that interacts with SYNV P3 (Min et al., 2010). Although the *A. thaliana* VOZ1 is expressed in phloem tissue (Mitsuda et al., 2004), a similar transcriptional activator is associated with or tethered to microtubules in *N. benthamiana* (Min et al., 2010; this study), like other plant and animal transcriptional activators (Hamada et al., 2009; Jackman et al., 2009). Our results suggest that TVCV P30 and LNYV P3 interaction with NbVOZ1 may be associated with aiding virus movement. This is supported by the findings that LNYV P3 and TVCV P30 lost both cell-to-cell movement *trans*-complementation activity and interaction with NbVOZ1 when the aspartic acid residue in the LxD/N_{50-70}G motif was mutated to alanine (Figs. 4 and 7). This correlation leads us to hypothesize that loss of movement function may be connected to the mutation of the D residue. We propose, that the transcriptional activator NbVOZ1, as suggested previously for SYNV P3 (Min et al., 2010), may be utilized by some MP to anchor virus movement complexes to the microtubule network for intracellular trafficking. Interaction with NbVOZ1 may be a common feature for certain 30K MP and perhaps could form the basis for a new subgrouping system for 30K-like MP. Future research may investigate the effect on virus movement when NbVOZ1 expression is knocked down by techniques like VIGS (Ruiz et al., 1998) or targeted genome modification using CRISPR-Cas (Shan et al., 2013).

Although ADV P3 did not appear to interact with the microtubule-associated NbVOZ1, we observed that it appeared to alter the largely microtubular distribution of NbVOZ1 (Fig. 6) into primarily a cell periphery pattern similar to when this MP is expressed alone. A potential host protein redistribution effect was also observed when ADV P3 was co-expressed with PDLP1 (Supplementary Fig. 3). ADV P3ΔMP similarly appeared to change the cellular distribution of PDLP1 and NbVOZ1 proteins, suggesting that mutation of the D residue in the 30K-specific LxD/N_{50-70}G motif is likely unrelated to this effect. One possible explanation for the altered cellular distribution of these membrane-localizing proteins could be that ADV P3 remodels host endomembranes through the actin network (Sparkes et al., 2009) similar to PVX TGB1 MP which was shown to reorganize host actin and endomembranes into viral replication complexes (Tilsner et al., 2012). Supporting a potential role in viral replication, ADV P3 was recently shown to interact with ADV phosphoprotein P (Bejerman et al., 2015), which is one of the core proteins of the rhabdoviral replication complex (Dietzgen, 2012). Since PVX requires the actin network for cell-to-cell movement, unlike TVCV (Harries et al., 2009), it is tempting to speculate that the actin network rather than microtubules may play a more central role in ADV P3-mediated cell-to-cell movement. This would explain why ADV P3 poorly supported TVCV movement and failed to interact with the microtubule-associated NbVOZ1 protein. Future studies will aim to investigate the detailed viral movement mechanisms associated with ADV P3.

Although secondary structure analysis helps to predict movement function (Huang et al., 2005), conflicting views have arisen as to the validity of some proposed plant rhabdoviral 30K superfamily candidates (Mushegian and Elena, 2015). Our results support the validity of identifying 30K MP candidates by analyzing the effect that D to A mutation in the LxD/N_{50-70}G motif has on movement function (Mushegian and Elena, 2015; Yu et al., 2013). Future studies should also consider the potential role of the nucleus in supporting plant rhabdovirus movement. Previous studies have shown that some viral MP such as rice stripe tenuivirus P2, PMTV TGB1 and groundnut rosette umbravirus ORF3 require nuclear host factors to support cell-to-cell movement (Kim

et al., 2007; Wright et al., 2010; Zheng et al., 2015). This observation may have relevance for LNYV P3, ADV P3, and TVCV P30 MP that localize at least partially to the nucleus in transient expression assays (Bejerman et al., 2015; Levy et al., 2013; Martin et al., 2012).

Methods

Generation of MP mutants

LNYV P3 and ADV P3 ORF (Bejerman et al., 2015; Martin et al., 2012) in pDONR221 (Life Technologies, California, USA) and TVCV P30 in pICH-17388 or pDONR221 (Fig. 1) were used as templates to generate MP-defective (ΔMP) constructs using the Q5®Site-Directed Mutagenesis Kit (New England Biolabs, MA, USA) following the manufacturer's instructions. Mutagenic primers were generated using the online program NEBaseChanger (New England Biolabs) following the recommendations for substitution primers (see Supplementary Table 3 for a list of primers used). Successful mutagenesis was validated by Sanger DNA sequencing by the Australian Genome Research Facility (AGRF, Brisbane).

Gateway cloning

MP-autofluorescent protein fusion constructs were generated by individually recombining the functional and mutated MP (LNYV P3, ADV P3, and TVCV P30) available in pDONR221 into RFP-, GFP- and BiFC-, pSITE plant expression vectors (kindly provided by Michael Goodin, University of Kentucky, USA) following the instructions of the Gateway LR Clonase II Enzyme Mix Kit (Life Technologies). LNYV and ADV N gene ORFs were cloned as previously described (Bejerman et al., 2015; Mann et al., 2015). *N. benthamiana* VOZ1 (1, 429 nt) and *A. thaliana* PDLP1 (1, 213 nt; accession number NM_123765.2) were amplified (See Supplementary Table 3 for primers used) from total RNA using a Plant Mini Kit following the manufacturer's instructions (Qiagen, Venlo, Netherlands). PCR amplicons were cloned into pGEM-T Easy (Promega, Madison, USA) and recombined into pSITE plant expression vectors as previously described (Goodin et al., 2007a; Mann et al., 2015).

Agroinfiltration of N. benthamiana plants

Wild-type and CFP-H2B transgenic (Martin et al., 2009) *N. benthamiana* plants were grown in glasshouse conditions at 25 °C with 16 h photoperiod. Four- to five-week old plants were infiltrated with agrobacterium GV3101 cultures following a previously reported protocol (Mann et al., 2015). For movement assays, all agrobacteria were initially resuspended in infiltration media to OD_{600} of 0.3. Subsequently, agrobacteria carrying TVCV pro-vector constructs (pICH-17388/*MP, pICH-7410 and pICH-14011; Fig. 1B) (Marillonnet et al., 2004) were mixed in equal proportions (v/v) and diluted to a final OD_{600} of 0.015 in 1 mL of agrobacteria culture carrying a putative MP in 35S:MP-RFP (Fig. 1B) (final OD_{600} 0.0015).

Localization and interaction assays and live cell imaging

For protein localization, agrobacteria cultures carrying GFP-MP fusion constructs were diluted to OD_{600} of 0.8 and then equal volumes were mixed with either aniline blue fluorochrome (Biosupplies Australia, Bundoora, VIC) solution [prepared by diluting the stock solution (0.1 mg/mL) 1:3 with water] or *A. thaliana* PDLP1-RFP. For BiFC protein–protein interaction assays, pSITE-BiFC-nEYFP-C1 and pSITE-BiFC-cEYFP-C1 vectors were used, where all viral proteins were expressed as C-terminal fusions to the amino- or carboxy-terminal portions of YFP. BiFC assays were carried out using cyan fluorescent nuclei (CFP-Histone 2B) transgenic marker plants (Martin et al., 2009). For localization and interaction assays, leaf samples from at least three leaves from each of three independent experiments were examined 2–3 days after agroinfiltration using a Zeiss LSM-700 confocal microscope at 40× magnification. Similarly, for movement complementation assays, leaf samples were viewed for GFP fluorescence 7 days postinfiltration at 10× magnification. All images were processed using Zen lite 2012 software (Carl Zeiss Microscopy, Germany).

Protein analysis

Soluble protein extracted from agroinfiltrated leaf tissue (20 mg) was resuspended in sample buffer (Laemmli, 1970) and separated on SDS – 12% polyacrylamide gels. Proteins were transferred to PVDF membrane (Millipore, Massachusetts, USA) and detected using anti-GFP antibodies as previously described (Mann et al., 2015). Protein sizes were estimated using the PageRuler pre-stained protein ladder (Thermo Scientific, Massachusetts, USA).

In silico analysis

MP amino acid sequences were analyzed using PROMALS3D (Pei and Grishin, 2014) and subsequent alignments were processed using Jalview (University of Dundee, Scotland) (www.jalview.org) and exported as “esp” files for image preparation.

Acknowledgments

We thank Prof. Bernard Carroll (The University of Queensland) for access to the TVCV pro-vector system (kindly provided by Dr. Victor Klimyuk, Icon Genetics, Halle, Germany) and advice, and A/Prof. Michael Goodin (University of Kentucky) for pSITE vectors, *N. benthamiana* marker line (CFP-H2B), primer information for amplification of SYNV sc4i21 and a critical read of the manuscript. N.B. was supported by a postdoctoral fellowship from INTA, Argentina (Grant 1029/2012). This research was jointly supported by the Queensland Department of Agriculture and Fisheries, the University of Queensland and by Australian Research Council Grant LP110100047.

Appendix A. Supplementary material

Supplementary data associated with this article can be found in the online version at http://dx.doi.org/10.1016/j.virol.2015.11.028.

References

Agranovsky, A.A., Folimonov, A.S., Folimonova, S., Morozov, S., Schiemann, J., Lesemann, D., Atabekov, J.G., 1998. Beet yellows closterovirus HSP70-like protein mediates the cell-to-cell movement of a potexvirus transport-deficient mutant and a hordeivirus-based chimeric virus. J. Gen. Virol. 79, 889–895.

Ajjikuttira, P., Loh, C.S., Wong, S.M., 2005. Reciprocal function of movement proteins and complementation of long-distance movement of Cymbidium mosaic virus RNA by Odontoglossum ringspot virus coat protein. J. Gen. Virol. 86, 1543–1553.

Amari, K., Boutant, E., Hofmann, C., Schmitt-Keichinger, C., Fernandez-Calvino, L., Didier, P., Lerich, A., Mutterer, J., Thomas, C.L., Heinlein, M., Mely, Y., Maule, A.J., Ritzenthaler, C., 2010. A family of plasmodesmal proteins with receptor-like properties for plant viral movement proteins. PLoS Pathog. 6, e1001119.

Amari, K., Lerich, A., Schmitt-Keichinger, C., Dolja, V.V., Ritzenthaler, C., 2011. Tubule-guided cell-to-cell movement of a plant virus requires class XI myosin motors. PLoS Pathog. 7, e1002327.

Ashby, J., Boutant, E., Seemanpillai, M., Groner, A., Sambade, A., Ritzenthaler, C., Heinlein, M., 2006. Tobacco mosaic virus movement protein functions as a structural microtubule-associated protein. J. Virol. 80, 8329–8344.
Bandyopadhyay, A., Kopperud, K., Anderson, G., Martin, K., Goodin, M., 2010. An integrated protein localization and interaction map for *Potato yellow dwarf virus*, type species of the genus *Nucleorhabdovirus*. Virology 402, 61–71.
Bejerman, N., Giolitti, F., de Breuil, S., Trucco, V., Nome, C., Lenardon, S., Dietzgen, R. G., 2015. Complete genome sequence and integrated protein localization and interaction map for alfalfa dwarf virus, which combines properties of both cytoplasmic and nuclear plant rhabdoviruses. Virology 483, 275–283.
Bertens, P., Wellink, J., Goldbach, R., van Kammen, A., 2000. Mutational analysis of the cowpea mosaic virus movement protein. Virology 267, 199–208.
Boutant, E., Fitterer, C., Ritzenthaler, C., Heinlein, M., 2009. Interaction of the tobacco mosaic virus movement protein with microtubules during the cell cycle in tobacco BY-2 cells. Protoplasma 237, 3–12.
Boyko, V., Hu, Q., Seemanpillai, M., Ashby, J., Heinlein, M., 2007. Validation of microtubule-associated tobacco mosaic virus RNA movement and involvement of microtubule-aligned particle trafficking. Plant J. 51, 589–603.
Cho, S.Y., Cho, W.K., Choi, H.S., Kim, K.H., 2012. Cis-acting element (SL1) of potato virus X controls viral movement by interacting with the NbMPB2Cb and viral proteins. Virology 427, 166–176.
Citovsky, V., Knorr, D., Schuster, G., Zambryski, P., 1990. The P30 movement protein of tobacco mosaic virus is a single-strand nucleic acid binding protein. Cell 60, 637–647.
Deom, C.M., He, X.Z., 1997. Second-site reversion of a dysfunctional mutation in a conserved region of the tobacco mosaic tobamovirus movement protein. Virology 232, 13–18.
Dietzgen, R.G., 2012. Morphology, genome organization, transcription and replication of rhabdoviruses. In: Dietzgen, R.G., Kuzmin, I.V. (Eds.), Rhabdoviruses: Molecular Taxonomy, Evolution, Genomics, Ecology, Host–vector Interactions, Cytopathology and Control. Caister Academic Press, Norfolk, UK, pp. 5–12.
Dietzgen, R.G., Callaghan, B., Wetzel, T., Dale, J.L., 2006. Completion of the genome sequence of *Lettuce necrotic yellows virus*, type species of the genus *Cytorhabdovirus*. Virus Res. 118, 16–22.
Dietzgen, R.G., Hunter, B.G., Francki, R.I.B., Jackson, A.O., 1989. Cloning of lettuce necrotic yellows virus RNA and identification of virus-specific polyadenylated RNAs in infected *Nicotiana glutinosa* leaves. J. Gen. Virol. 70, 2299–2307.
Dietzgen, R.G., Kuhn, J.H., Clawson, A.N., Freitas-Astua, J., Goodin, M.M., Kitajima, E. W., Kondo, H., Wetzel, T., Whitfield, A.E., 2014. *Dichorhavirus*: a proposed new genus for *Brevipalpus* mite-transmitted, nuclear, bacilliform, bipartite, negative-strand RNA plant viruses. Arch. Virol. 159, 607–619.
Dietzgen, R.G., Martin, K.M., Anderson, G., Goodin, M.M., 2012. *In planta* localization and interactions of impatiens necrotic spot tospovirus proteins. J. Gen. Virol. 93, 2490–2495.
Ding, B., Haudenshield, J.S., Hull, R.J., Wolf, S., Beachy, R.N., Lucas, W.J., 1992. Secondary plasmodesmata are specific sites of localization of the tobacco mosaic virus movement protein in transgenic tobacco plants. Plant Cell 4, 915–928.
Ferralli, J., Ashby, J., Fasler, M., Boyko, V., Heinlein, M., 2006. Disruption of microtubule organization and centrosome function by expression of tobacco mosaic virus movement protein. J. Virol. 80, 5807–5821.
Giesman-Cookmeyer, D., Silver, S., Vaewhongs, A.A., Lommel, S.A., Deom, C.M., 1995. Tobamovirus and dianthovirus movement proteins are functionally homologous. Virology 213, 38–45.
Giritch, A., Marillonnet, S., Engler, C., van Eldik, G., Botterman, J., Klimyuk, V., Gleba, Y., 2006. Rapid high-yield expression of full-size IgG antibodies in plants coinfected with noncompeting viral vectors. Proc. Natl. Acad. Sci. USA 103, 14701–14706.
Goodin, M.M., Chakrabarty, R., Banerjee, R., Yelton, S., Debolt, S., 2007a. New gateways to discovery. Plant Physiol. 145, 1100–1109.
Goodin, M.M., Chakrabarty, R., Yelton, S., Martin, K., Clark, A., Brooks, R., 2007b. Membrane and protein dynamics in live plant nuclei infected with *Sonchus yellow net virus*, a plant-adapted rhabdovirus. J. Gen. Virol. 88, 1810–1820.
Hamada, T., Igarashi, H., Taguchi, R., Fujiwara, M., Fukao, Y., Shimmen, T., Yokota, E., Sonobe, S., 2009. The putative RNA-processing protein, THO2, is a microtubule-associated protein in tobacco. Plant Cell Physiol. 50, 801–811.
Harries, P.A., Park, J.W., Sasaki, N., Ballard, K.D., Maule, A.J., Nelson, R.S., 2009. Differing requirements for actin and myosin by plant viruses for sustained intercellular movement. Proc. Natl. Acad. Sci. USA 106, 17594–17599.
Heim, F., Lot, H., Delecolle, B., Bassler, A., Krczal, G., Wetzel, T., 2008. Complete nucleotide sequence of a putative new cytorhabdovirus infecting lettuce. Arch. Virol. 153, 81–92.
Heinlein, M., Padgett, H.S., Gens, J.S., Pickard, B.G., Casper, S.J., Epel, B.L., Beachy, R. N., 1998a. Changing patterns of localization of the tobacco mosaic virus movement protein and replicase to the endoplasmic reticulum and microtubules during infection. Plant Cell 10, 1107–1120.
Heinlein, M., Wood, M.R., Thiel, T., Beachy, R.N., 1998b. Targeting and modification of prokaryotic cell–cell junctions by tobacco mosaic virus cell-to-cell movement protein. Plant J. 14, 345–351.
Hiraguri, A., Hibino, H., Hayashi, T., Netsu, O., Shimizu, T., Uehara-Ichiki, T., Omura, T., Sasaki, N., Nyunoya, H., Sasaya, T., 2012. The movement protein encoded by gene 3 of rice transitory yellowing virus is associated with virus particles. J. Gen. Virol. 93, 2290–2298.
Hiraguri, A., Hibino, H., Hayashi, T., Shimizu, T., Uehara-Ichiki, T., Omura, T., Sasaya, T., 2010. Complete sequence analysis of rice transitory yellowing virus and its comparison to rice yellow stunt virus. Arch. Virol. 155, 243–245.
Huang, Y.W., Geng, Y.F., Ying, X.B., Chen, X.Y., Fang, R.X., 2005. Identification of a movement protein of rice yellow stunt rhabdovirus. J. Virol. 79, 2108–2114.
Ishikawa, K., Maejima, K., Komatsu, K., Netsu, O., Keima, T., Shiraishi, T., Okano, Y., Hashimoto, M., Yamaji, Y., Namba, S., 2013. Fig mosaic emaravirus p4 protein is involved in cell-to-cell movement. J. Gen. Virol. 94, 682–686.
Jackman, R.W., Rhoads, M.G., Cornwell, E., Kandarian, S.C., 2009. Microtubule-mediated NF-kappaB activation in the TNF-alpha signaling pathway. Exp. Cell Res. 315, 3242–3249.
Jackson, A.O., Dietzgen, R.G., Goodin, M.M., Bragg, J.N., Deng, M., 2005. Biology of plant rhabdoviruses. Annu. Rev. Phytopathol. 43, 623–660.
Kahn, T.W., Lapidot, M., Heinlein, M., Reichel, C., Cooper, B., Gafny, R., Beachy, R.N., 1998. Domains of the TMV movement protein involved in subcellular localization. Plant J. 15, 15–25.
Karasev, A.V., Kashina, A.S., Gelfand, V.I., Dolja, V.V., 1992. HSP70-related 65 kDa protein of beet yellows closterovirus is a microtubule-binding protein. FEBS Lett. 304, 12–14.
Kasteel, D.T., Perbal, M.C., Boyer, J.C., Wellink, J., Goldbach, R.W., Maule, A.J., van Lent, J.W., 1996. The movement proteins of cowpea mosaic virus and cauliflower mosaic virus induce tubular structures in plant and insect cells. J. Gen. Virol. 77, 2857–2864.
Kim, S.H., Macfarlane, S., Kalinina, N.O., Rakitina, D.V., Ryabov, E.V., Gillespie, T., Haupt, S., Brown, J.W., Taliansky, M., 2007. Interaction of a plant virus-encoded protein with the major nucleolar protein fibrillarin is required for systemic virus infection. Proc. Natl. Acad. Sci. USA 104, 11115–11120.
Koonin, E.V., Mushegian, A.R., Ryabov, E.V., Dolja, V.V., 1991. Diverse groups of plant RNA and DNA viruses share related movement proteins that may possess chaperone-like activity. J. Gen. Virol. 72, 2895–2903.
Laemmli, U.K., 1970. Cleavage of structural proteins during the assembly of the head of bacteriophage T4. Nature 227, 680–685.
Laporte, C., Vetter, G., Loudes, A.M., Robinson, D.G., Hillmer, S., Stussi-Garaud, C., Ritzenthaler, C., 2003. Involvement of the secretory pathway and the cytoskeleton in intracellular targeting and tubule assembly of grapevine fanleaf virus movement protein in tobacco BY-2 cells. Plant Cell 15, 2058–2075.
Lauber, E., Bleykasten-Grosshans, C., Erhardt, M., Bouzoubaa, S., Jonard, G., Richards, K.E., Guilley, H., 1998. Cell-to-cell movement of beet necrotic yellow vein virus: I. Heterologous complementation experiments provide evidence for specific interactions among the triple gene block proteins. Mol. Plant-Microbe Interact. 11, 618–625.
Lazarowitz, S.G., Beachy, R.N., 1999. Viral movement proteins as probes for intracellular and intercellular trafficking in plants. Plant Cell 11, 535–548.
Levy, A., Zheng, J.Y., Lazarowitz, S.G., 2013. The tobamovirus turnip vein clearing virus 30-kilodalton movement protein localizes to novel nuclear filaments to enhance virus infection. J. Virol. 87, 6428–6440.
Lewandowski, D.J., Adkins, S., 2005. The tubule-forming NSm protein from tomato spotted wilt virus complements cell-to-cell and long-distance movement of tobacco mosaic virus hybrids. Virology 342, 26–37.
Li, W., Lewandowski, D.J., Hilf, M.E., Adkins, S., 2009. Identification of domains of the tomato spotted wilt virus NSm protein involved in tubule formation, movement and symptomatology. Virology 390, 110–121.
Li, Y., Bao, Y.M., Wei, C.H., Kang, Z.S., Zhong, Y.W., Mao, P., Wu, G., Chen, Z.L., Schiemann, J., Nelson, R.S., 2004. Rice dwarf phytoreovirus segment S6-encoded nonstructural protein has a cell-to-cell movement function. J. Virol. 78, 5382–5389.
Liu, C., Nelson, R.S., 2013. The cell biology of tobacco mosaic virus replication and movement. Front. Plant Sci. 4.
Mann, K.S., Dietzgen, R.G., 2014. Plant rhabdoviruses: new insights and research needs in the interplay of negative-strand RNA viruses with plant and insect hosts. Arch. Virol. 159, 1889–1900.
Mann, K.S., Johnson, K.N., Dietzgen, R.G., 2015. Cytorhabdovirus phosphoprotein shows RNA silencing suppressor activity in plants, but not in insect cells. Virology 476, 413–418.
Marillonnet, S., Giritch, A., Gils, M., Kandzia, R., Klimyuk, V., Gleba, Y., 2004. *In planta* engineering of viral RNA replicons: efficient assembly by recombination of DNA modules delivered by Agrobacterium. Proc. Natl. Acad. Sci. USA 101, 6852–6857.
Marillonnet, S., Thoeringer, C., Kandzia, R., Klimyuk, V., Gleba, Y., 2005. Systemic *Agrobacterium tumefaciens*-mediated transfection of viral replicons for efficient transient expression in plants. Nat. Biotechnol. 23, 718–723.
Martin, K., Kopperud, K., Chakrabarty, R., Banerjee, R., Brooks, R., Goodin, M.M., 2009. Transient expression in *Nicotiana benthamiana* fluorescent marker lines provides enhanced definition of protein localization, movement and interactions in planta. Plant J. 59, 150–162.
Martin, K.M., Dietzgen, R.G., Wang, R., Goodin, M.M., 2012. Lettuce necrotic yellows cytorhabdovirus protein localization and interaction map, and comparison with nucleorhabdoviruses. J. Gen. Virol. 93, 906–914.
Massah, A., Izadpanah, K., Afsharifar, A.R., Winter, S., 2008. Analysis of nucleotide sequence of Iranian maize mosaic virus confirms its identity as a distinct nucleorhabdovirus. Arch. Virol. 153, 1041–1047.
Melcher, U., 2000. The '30K' superfamily of viral movement proteins. J. Gen. Virol. 81, 257–266.
Min, B.E., Martin, K., Wang, R., Tafelmeyer, P., Bridges, M., Goodin, M., 2010. A host-factor interaction and localization map for a plant-adapted rhabdovirus implicates cytoplasm-tethered transcription activators in cell-to-cell movement. Mol. Plant-Microbe Interact. 23, 1420–1432.
Mise, K., Allison, R.F., Janda, M., Ahlquist, P., 1993. Bromovirus movement protein genes play a crucial role in host specificity. J. Virol. 67, 2815–2823.

Mitsuda, N., Hisabori, T., Takeyasu, K., Sato, M.H., 2004. VOZ; isolation and characterization of novel vascular plant transcription factors with a one-zinc finger from *Arabidopsis thaliana*. Plant Cell Physiol. 45, 845–854.
Morozov, S., Fedorkin, O.N., Juttner, G., Schiemann, J., Baulcombe, D.C., Atabekov, J. G., 1997. Complementation of a potato virus X mutant mediated by bombardment of plant tissues with cloned viral movement protein genes. J. Gen. Virol. 78, 2077–2083.
Mushegian, A.R., Elena, S.F., 2015. Evolution of plant virus movement proteins from the 30K superfamily and of their homologs integrated in plant genomes. Virology 476, 304–315.
Niehl, A., Pasquier, A., Ferriol, I., Mely, Y., Heinlein, M., 2014. Comparison of the oilseed rape mosaic virus and tobacco mosaic virus movement proteins (MP) reveals common and dissimilar MP functions for tobamovirus spread. Virology 456, 43–54.
Niehl, A., Pena, E.J., Amari, K., Heinlein, M., 2013. Microtubules in viral replication and transport. Plant J. 75, 290–308.
Oparka, K.J., Prior, D.A., Santa Cruz, S., Padgett, H.S., Beachy, R.N., 1997. Gating of epidermal plasmodesmata is restricted to the leading edge of expanding infection sites of tobacco mosaic virus (TMV). Plant J. 12, 781–789.
Padgett, H.S., Epel, B.L., Kahn, T.W., Heinlein, M., Watanabe, Y., Beachy, R.N., 1996. Distribution of tobamovirus movement protein in infected cells and implications for cell-to-cell spread of infection. Plant J. 10, 1079–1088.
Pei, J., Grishin, N.V., 2014. PROMALS3D: multiple protein sequence alignment enhanced with evolutionary and three-dimensional structural information. Methods Mol. Biol. 1079, 263–271.
Reed, S.E., Tsai, C.W., Willie, K.J., Redinbaugh, M.G., Hogenhout, S.A., 2005. Shotgun sequencing of the negative-sense RNA genome of the rhabdovirus Maize mosaic virus. J. Virol. Methods 129, 91–96.
Revill, P., Trinh, X., Dale, J., Harding, R., 2005. Taro vein chlorosis virus: characterization and variability of a new nucleorhabdovirus. J. Gen. Virol. 86, 491–499.
Robards, A.W., Lucas, W.J., 1990. Plasmodesmata. Annu. Rev. Plant Physiol. Plant Mol. Biol. 41, 369–419.
Ruiz, M.T., Voinnet, O., Baulcombe, D.C., 1998. Initiation and maintenance of virus-induced gene silencing. Plant Cell 10, 937–946.
Ryabov, E.V., Oparka, K.J., Santa Cruz, S., Robinson, D.J., Taliansky, M.E., 1998. Intracellular location of two groundnut rosette umbravirus proteins delivered by PVX and TMV vectors. Virology 242, 303–313.
Sasaki, N., Park, J.W., Maule, A.J., Nelson, R.S., 2006. The cysteine-histidine-rich region of the movement protein of cucumber mosaic virus contributes to plasmodesmal targeting, zinc binding and pathogenesis. Virology 349, 396–408.
Schoen, C.D.L., W., Moller, I., Groeneveld, L., Klerks, M.M., Lindner, J.L., 2004. The complete genomic sequence of strawberry crinkle virus, a member of the *Rhabdoviridae*. Acta Hortic. 656, 45–50.
Scholthof, H.B., 2005. Plant virus transport: motions of functional equivalence. Trends Plant Sci. 10, 376–382.
Scholthof, K.B., Hillman, B.I., Modrell, B., Heaton, L.A., Jackson, A.O., 1994. Characterization and detection of sc4: a sixth gene encoded by sonchus yellow net virus. Virology 204, 279–288.
Sevilem, I., Miyashima, S., Helariutta, Y., 2013. Cell-to-cell communication via plasmodesmata in vascular plants. Cell. Adhes. Migr. 7, 27–32.
Shan, Q., Wang, Y., Li, J., Zhang, Y., Chen, K., Liang, Z., Zhang, K., Liu, J., Xi, J.J., Qiu, J.-L., Gao, C., 2013. Targeted genome modification of crop plants using a CRISPR-Cas system. Nature Biotech. 31, 686–688.
Solovyev, A.G., Zelenina, D.A., Savenkov, E.I., Grdzelishvili, V.Z., Morozov, S.Y., Lesemann, D.E., Maiss, E., Casper, R., Atabekov, J.G., 1996. Movement of a barley stripe mosaic virus chimera with a tobacco mosaic virus movement protein. Virology 217, 435–441.
Sparkes, I., Runions, J., Hawes, C., Griffing, L., 2009. Movement and remodeling of the endoplasmic reticulum in nondividing cells of tobacco leaves. Plant Cell 21, 3937–3949.
Storms, M.M., Kormelink, R., Peters, D., Van Lent, J.W., Goldbach, R.W., 1995. The nonstructural NSm protein of tomato spotted wilt virus induces tubular structures in plant and insect cells. Virology 214, 485–493.
Tamai, A., Kubota, K., Nagano, H., Yoshii, M., Ishikawa, M., Mise, K., Meshi, T., 2003. Cucumovirus- and bromovirus-encoded movement functions potentiate cell-to-cell movement of tobamo- and potexviruses. Virology 315, 56–67.
Tanno, F., Nakatsu, A., Toriyama, S., Kojima, M., 2000. Complete nucleotide sequence of Northern cereal mosaic virus and its genome organization. Arch. Virol. 145, 1373–1384.
Thomas, C.L., Maule, A.J., 1995. Identification of structural domains within the cauliflower mosaic virus movement protein by scanning deletion mutagenesis and epitope tagging. Plant Cell 7, 561–572.
Tilsner, J., Cowan, G.H., Roberts, A.G., Chapman, S.N., Ziegler, A., Savenkov, E., Torrance, L., 2010. Plasmodesmal targeting and intercellular movement of potato mop-top pomovirus is mediated by a membrane anchored tyrosine-based motif on the lumenal side of the endoplasmic reticulum and the C-terminal transmembrane domain in the TGB3 movement protein. Virology 402, 41–51.
Tilsner, J., Linnik, O., Wright, K.M., Bell, K., Roberts, A.G., Lacomme, C., Santa Cruz, S., Oparka, K.J., 2012. The TGB1 movement protein of potato virus X reorganizes actin and endomembranes into the X-body, a viral replication factory. Plant Physiol. 158, 1359–1370.
Tilsner, J., Taliansky, M., Torrance, L., 2014. Plant virus movement. eLS, 1–12. http://dx.doi.org/10.1002/9780470015902.a0020711.pub2.
Tomenius, K., Clapham, D., Meshi, T., 1987. Localization by immunogold cytochemistry of the virus-coded 30K protein in plasmodesmata of leaves infected with tobacco mosaic virus. Virology 160, 363–371.
Tsai, C.W., Redinbaugh, M.G., Willie, K.J., Reed, S., Goodin, M., Hogenhout, S.A., 2005. Complete genome sequence and in planta subcellular localization of maize fine streak virus proteins. J. Virol. 79, 5304–5314.
Walker, P.J., Dietzgen, R.G., Joubert, D.A., Blasdell, K.R., 2011. Rhabdovirus accessory genes. Virus Res. 162, 110–125.
Wang, Q., Ma, X., Qian, S., Zhou, X., Sun, K., Chen, X., Zhou, X., Jackson, A.O., Li, Z., 2015. Rescue of a plant negative-strand RNA virus from cloned cDNA: insights into enveloped plant virus movement and morphogenesis. PLoS Pathog. 11, e1005223.
Wolf, S., Deom, C.M., Beachy, R.N., Lucas, W.J., 1989. Movement protein of tobacco mosaic virus modifies plasmodesmatal size exclusion limit. Science 246, 377–379.
Wright, K.M., Cowan, G.H., Lukhovitskaya, N.I., Tilsner, J., Roberts, A.G., Savenkov, E. I., Torrance, L., 2010. The N-terminal domain of PMTV TGB1 movement protein is required for nucleolar localization, microtubule association, and long-distance movement. Mol. Plant-Microbe Interact. 23, 1486–1497.
Wright, K.M., Wood, N.T., Roberts, A.G., Chapman, S., Boevink, P., Mackenzie, K.M., Oparka, K.J., 2007. Targeting of TMV movement protein to plasmodesmata requires the actin/ER network: evidence from FRAP. Traffic 8, 21–31.
Yu, C., Karlin, D.G., Lu, Y., Wright, K., Chen, J., MacFarlane, S., 2013. Experimental and bioinformatic evidence that raspberry leaf blotch emaravirus P4 is a movement protein of the 30K superfamily. J. Gen. Virol. 94, 2117–2128.
Zhang, C., Machray, G.C., Cruz, S.S., Wilson, T.M.A., 2005. Soil-borne wheat mosaic virus (SBWMV) 37 kDa protein rescues cell-to-cell and long-distance movement of an immobile tobacco mosaic virus mutant in *Nicotiana benthamiana*, a non-host of SBWMV. J. Phytopathol. 153, 5–10.
Zhang, C., Pei, X., Wang, Z., Jia, S., Guo, S., Zhang, Y., Li, W., 2012. The Rice stripe virus pc4 functions in movement and foliar necrosis expression in *Nicotiana benthamiana*. Virology 425, 113–121.
Zheng, L., Du, Z., Lin, C., Mao, Q., Wu, K., Wu, J., Wei, T., Wu, Z., Xie, L., 2015. Rice stripe tenuivirus p2 may recruit or manipulate nucleolar functions through an interaction with fibrillarin to promote virus systemic movement. Mol. Plant Pathol. 16, 921–930.
Ziegler-Graff, V., Guilford, P.J., Baulcombe, D.C., 1991. Tobacco rattle virus RNA-1 29K gene product potentiates viral movement and also affects symptom induction in tobacco. Virology 182, 145–155.